



1 The role of catchment characteristics, discharge, and active layer thaw on seasonal stream chemistry
2 across ten permafrost catchments.

3

4 Authors: Arsh Grewal¹, Erin M. Nicholls², Sean K. Carey¹

5 ¹School of Earth, Environment, and Society, McMaster University, ON, Canada

6 ²Department of Earth, Energy, and Environment, University of Calgary, AB, Canada

7 **Corresponding Author:** Arsh Grewal, akgrewal@mcmaster.ca

8 **Corresponding Author Present Address:** Department of Earth & Environmental Sciences, Michigan State
9 University, MI, United States, grewala7@msu.edu

10 Keywords: Watershed Hydrology, Concentration-Discharge, Permafrost Hydrology, Water Quality,
11 Permafrost, Solute Export,

12

13

14

15



16 Abstract

17 High latitude catchments are rapidly warming, leading to altered precipitation regimes, widespread
18 permafrost degradation and observed shifts in stream chemistry for major arctic rivers. At headwater
19 scales, stream discharge and chemistry are seasonally variable, and the relative influence of catchment
20 characteristics, climate and active layer thaw on this seasonality has been poorly addressed. To provide
21 new insight into mechanisms driving changes in streamflow chemistry within permafrost watersheds, we
22 measured discharge and sampled major ion and dissolved organic carbon (DOC) concentrations across
23 ten permafrost catchments in Yukon Territory, Canada. We incorporated concentration-discharge
24 relationships within generalized additive models to resolve the distinct influence of discharge and
25 seasonal active layer thaw on stream chemistry and identify the role of watershed characteristics on the
26 magnitude and seasonality of solute concentrations. After accounting for seasonal variations in
27 discharge, results indicate both major ions and DOC were highly seasonal across all catchments, with
28 DOC declining and major ion concentration increasing post freshet. Seasonal variability in major ion
29 concentrations were primarily driven by active layer thaw, whereas DOC seasonality was strongly
30 controlled by flushing of soil organic carbon during freshet. While major ion concentrations were
31 geologically mediated, greater permafrost extent led to enhanced seasonality in major ion
32 concentrations. Catchments with strong topographical gradients and thinner organic soils had higher
33 specific discharge, lower DOC concentrations but greater relative seasonality. Our results highlight the
34 important role catchment characteristics play on shaping both the seasonal variations and magnitude of
35 solute concentrations in permafrost underlain watersheds.

36 1. Introduction

37 High latitude catchments are experiencing rapid warming due to polar amplification (Cohen et al., 2014),
38 and are highly sensitive as thawing permafrost and altered precipitation regimes strongly affect their
39 hydrological and biogeochemical cycles (McKenzie et al., 2021; Walvoord and Kurylyk, 2016). Frozen
40 ground and permafrost act as impeding layers to water movement, restricting flow and separating supra,
41 intra and sub-permafrost aquifers (McKenzie et al., 2021; Woo, 1986). Where present, permafrost
42 enhances runoff by restricting deep percolation and encouraging flow through more hydraulically
43 conductive near-surface pathways (Carey and Woo, 2001; Quinton and Marsh, 1999; Woo and Steer,
44 1983). Permafrost degradation, which includes deepening of the seasonal thawed zone (termed the



45 active layer) and wholesale loss, also influences stream chemistry (Frey and McClelland, 2009; Walvoord
46 and Kurylyk, 2016). Dissolved solutes are expected to increase due to greater contact with mineral
47 surfaces as flow pathways lengthen. Vast stores of frozen organic material are thawing, yet dissolved
48 organic carbon (DOC) concentration projections are uncertain due to potential increased adsorption and
49 in-stream processes (Frey and McClelland, 2009; Tank et al., 2023). Studies from large arctic rivers show
50 increase exports of weathering products such as Ca, Mg and DOC (Tank et al., 2016), yet results are
51 varied across circumpolar regions (Tank et al., 2023), and long-term studies are limited to extremely
52 large rivers that cross multiple ecozones and permafrost extent, confounding interpretation.

53

54 Active layer dynamics along with seasonal precipitation (phase and magnitude) play a critical role in
55 runoff and solute export processes (McNamara et al., 1998; Woo and Winter, 1993). During spring, large
56 volumes of meltwater infiltrate the soil yet are restricted to near surface layers that are often organic,
57 exporting large volumes of water rich with dissolved organic matter (DOM; Carey, 2003; MacLean et al.,
58 1999; Shatilla et al., 2023; Woo and Steer, 1986). As the frost front descends, mineral layers thaw and
59 catchment storage increases resulting in greater concentrations of weathering solutes and reduced DOM
60 (Carey, 2003; Carey et al., 2013; Petrone et al., 2006). Concentrations of weathering derived solutes
61 generally increase from spring to fall, whereas DOM concentrations typically decrease (Carey, 2003; Frey
62 and Smith, 2005; MacLean et al., 1999). The position of the water table with respect to different soil
63 horizons in the active layer has largely been used to explain seasonal patterns of dissolved solutes in the
64 permafrost literature. Permafrost extent is also identified as a key driver of hydrological and
65 biogeochemical processes. For example, Petrone et al. (2006) and Webster et al. (2022) attributed lower
66 yield of NO_3^- and higher yield of fluorescent dissolved organic matter (fDOM) to greater permafrost
67 extent in Alaska. Webster et al. (2022) found evidence of greater seasonality of NO_3^- in high permafrost
68 catchments compared to catchments with lower permafrost extent.

69 Changes in hydrological connectivity across the landscape can alter streamflow chemistry and solute
70 export (Creed et al., 2015; Li et al., 2024; Zhi et al., 2019). During wet periods, water tables are near the
71 surface in highly conductive organic soils and areas distal to the stream can be connected. During drier
72 conditions, flow is primarily through deeper mineral pathways and landscape connectivity declines
73 (Stewart et al., 2022; Zhi et al., 2019). The presence and disposition of permafrost strongly affects the
74 interaction between solute sources, water pathways and the stream network. Direct observations of



75 these interactions are rare in northern watersheds as permafrost extent is often difficult to assess and
76 logistics are typically challenging. Concentration-Discharge (CQ) relations have increasingly been used to
77 characterize flow-solute coupling to infer catchment processes (Godsey et al., 2009; Hall, 1970; Wymore
78 et al., 2023). By comparing the log-log slope between the two, it is possible to characterize whether a
79 solute displays flushing behaviour (positive slope) or dilution (negative slope). Other metrics such as
80 $CV_C:CV_Q$ ratios can be used to determine whether a solute is chemostatic or chemodynamic even when
81 there is no clear directionality (Musolff et al., 2015; Thompson et al., 2011). Positive/negative slopes can
82 indicate spatial and vertical heterogeneity within a catchment, whereas slopes close to zero can indicate
83 homogeneity in vertical and spatial distribution of solute stores or dominance of instream
84 biogeochemical processes (Creed et al., 2015).

85 Active layer thaw and streamflow are highly seasonal in permafrost catchments, making it difficult to
86 ascertain the relative influence of each factor in driving seasonal solute dynamics. For example, major
87 ion concentrations typically increase throughout the ice-free season. This seasonality can be driven by
88 decreasing discharge, which can lower connectivity with the ion poor shallow organic layer. However,
89 thawing of active layer can also lead to greater water movement through the mineral layer, increasing
90 stream ion concentrations. The potential influence of both discharge and active layer dynamics on
91 seasonal stream chemistry in cold regions are rarely disentangled. Shifts in CQ relationships can be used
92 to detect changes in solute export driven by processes other than discharge, such as changes in the
93 internal structure of the catchment (i.e. ground freeze-thaw) or in the quantity/mobility of solute stores.
94 For example, Fork et al. (2020) examined changes in residuals of water flux versus DOC to infer changes
95 in supply in terrestrial pools of DOC. Biagi et al. (2022) and Ross et al. (2022) utilized generalized additive
96 models (GAMs), which are flexible models that allow for the addition of spline terms to model non-linear
97 behaviour, to quantify changes in CQ relationships over time in agricultural environments. CQ
98 relationships are often highly seasonal in northern catchments, particularly between snowmelt and
99 summer periods (MacLean et al., 1999; Shatilla et al., 2023). MacLean et al. (1999) compared CQ
100 patterns between seasons in a permafrost underlain Alaskan catchment, however the authors classified
101 each season and thus had to assume that the transition between seasons is a discreet phenomenon. At
102 the event scale, Shogren et al. (2021) found both seasonality and landscape drivers to be important for
103 the relations between DOC, NO_3^- and flow. The authors determined that landscape drivers were more
104 important to CQ relationships than seasonality for DOC and NO_3^- in Arctic catchments post freshet.



105 In cold catchments, seasonal patterns of freeze-thaw, discharge, and solute stores have been identified
106 as drivers for variability in stream chemistry (Boyer et al., 1997; Carey, 2003; MacLean et al., 1999;
107 Petrone et al., 2006). However, the relative importance of each factor and how it is influenced by
108 permafrost extent and other catchment characteristics remains unresolved. To address this, we
109 characterize CQ relationships using discrete major ion and DOC data across ten permafrost influenced
110 catchments. We utilize GAMs with an additional spline Day Of Year (sDOY) term to the traditional CQ
111 approach to test two hypotheses:

- 112 1. As active layer thaws, concentrations will increase for major ions and decrease for DOC at all
113 sites (irrespective of seasonal changes in discharge), due to seasonal ground thaw induced
114 activation of deeper mineral rich flow paths.
- 115 2. Seasonal changes in concentrations for both major ions and DOC will be the largest in
116 catchments with greater permafrost extent (irrespective of seasonality in discharge) due to
117 greater connectivity of subpermafrost water to streams in catchments with lower permafrost
118 extent.

119 Testing these hypotheses will provide new insights on the role of catchment characteristics and
120 permafrost extent on the seasonality of major ions and DOC export. By disentangling different drivers of
121 seasonal solute export in northern environments, we can make more informed predictions of stream
122 biogeochemistry in a rapidly changing north.

123 2. Data and Methods

124 2.1. Study Area

125 Our study consists of 10 catchments with areas ranging from $\sim 5 \text{ km}^2$ to $\sim 170 \text{ km}^2$, all located in Yukon
126 Territory, Canada. Four of the catchments are part of the Wolf Creek Research Basin (WCRB; $60^\circ 36' \text{ N}$,
127 $134^\circ 57' \text{ W}$; Figure 1), with WCRB outlet (WCO) being the largest. Coal Lake (CL) is a $\sim 70 \text{ km}^2$
128 subcatchment of WCRB that has a $\sim 1 \text{ km}^2$ well mixed lake near the outlet. Granger Creek (GC) and
129 Buckbrush Creek (BB) are alpine headwater subcatchments of WCRB and have areas less than 10 km^2 .
130 WCO and CL are underlain with sporadic permafrost (Lewkowicz and Ednie, 2004). Low elevation areas
131 of WCRB consist of primarily coniferous forests, whereas high elevation areas consist of shrub taiga and
132 alpine tundra vegetation. High elevation subcatchments (BB, GC) are estimated to be underlain by



133 discontinuous permafrost (Lewkowicz and Ednie, 2004) and are typically colder and wetter than low
134 elevation areas of WCRB. Near surface geology consists of mostly sedimentary rocks such as limestone,
135 sandstone, and siltstone capped by a till mantle and glaciofluvial/glaciolacustrine deposits (Rasouli et al.,
136 2014). WCRB is part of the traditional territories of the Ta'an Kwach'an Council, Kwanlin Dün, and
137 Carcross/Tagish First Nations. More detailed description of WCRB can be found in (Rasouli et al., 2014,
138 2019). Climate normals (1991-2020) reported near WCRB at the Whitehorse airport show the average air
139 temperature is 0.2 °C with an annual precipitation of 279.6 mm (164 mm as rain). Due to the large
140 elevation gradient at WCRB, average temperatures in the headwater regions are several degrees lower,
141 and precipitation volumes are larger, often exceeding 400 mm per year.

142

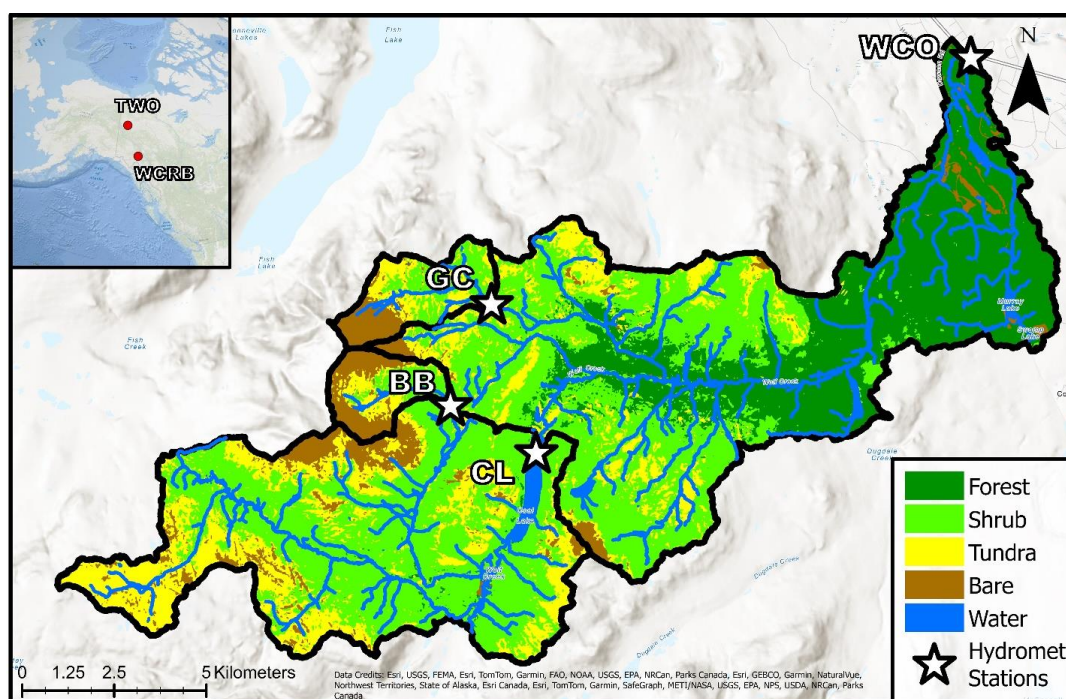
143 Six of our study catchments are part of the Tombstone Waters Observatory (TWO; Figure 2), which is
144 part of the traditional territory of Tr'ondëk Hwëch'in First Nation. All TWO catchments have areas less
145 than 35 km². All TWO catchments intersect the Dempster highway, a critical north-south road. All TWO
146 catchments are named after the kilometer marker where the stream intersects the highway. The six
147 catchments are called Km 44, Km 71, Km 99, Km 104, Km 175, and Km 185. Km 44 (64° 19' N, 138° 31' W)
148 and Km 71 (64° 31' N, 138° 8' W) are the most mountainous catchments, with strong topographic
149 gradients (Table 1). Km 44 primarily consists of bare earth, whereas Km 71 is largely overlain with shrub
150 cover. Km 99 and Km 104 (64° 41' N, 138° 28' W) are treeless catchments and are overlain by a thick
151 layer of peat except for the high elevation areas with steep slopes. Km 104 is largely flat, whereas Km 99
152 has mountainous uplands with more mineral soils. Km 175 (65° 12' N, 138° 26' W) and Km 185 (65° 16'
153 N, 138° 18' W) are primarily covered by open coniferous forests and are a part of the Ogilvie Mountain
154 range. Although there is some discrepancy between various permafrost mapping products in regard to
155 permafrost extent, the general consensus is that the WCRB sites have less permafrost than the TWO
156 sites (Bonnaventure et al., 2012; Obu et al., 2019; Ran et al., 2022; Surficial Geology dataset, 2024).
157 Surficial geology maps in TWO indicate that Km 71, Km 99, Km 104, and Km 185 are underlain with
158 continuous permafrost (>90%), whereas Km 44 is underlain with sporadic permafrost and Km 175 is
159 underlain with discontinuous permafrost (Thomas and Rampton, 1982a, b; Surficial Geology dataset,
160 2024). Climate normals (1991-2020) from Dawson City, the nearest Environment Canada weather station
161 to TWO, reports annual precipitation of 319 mm of which 208 mm is rainfall. The annual air temperature
162 is -3.8 °C. However, local climate can be quite variable amongst study catchments in TWO.



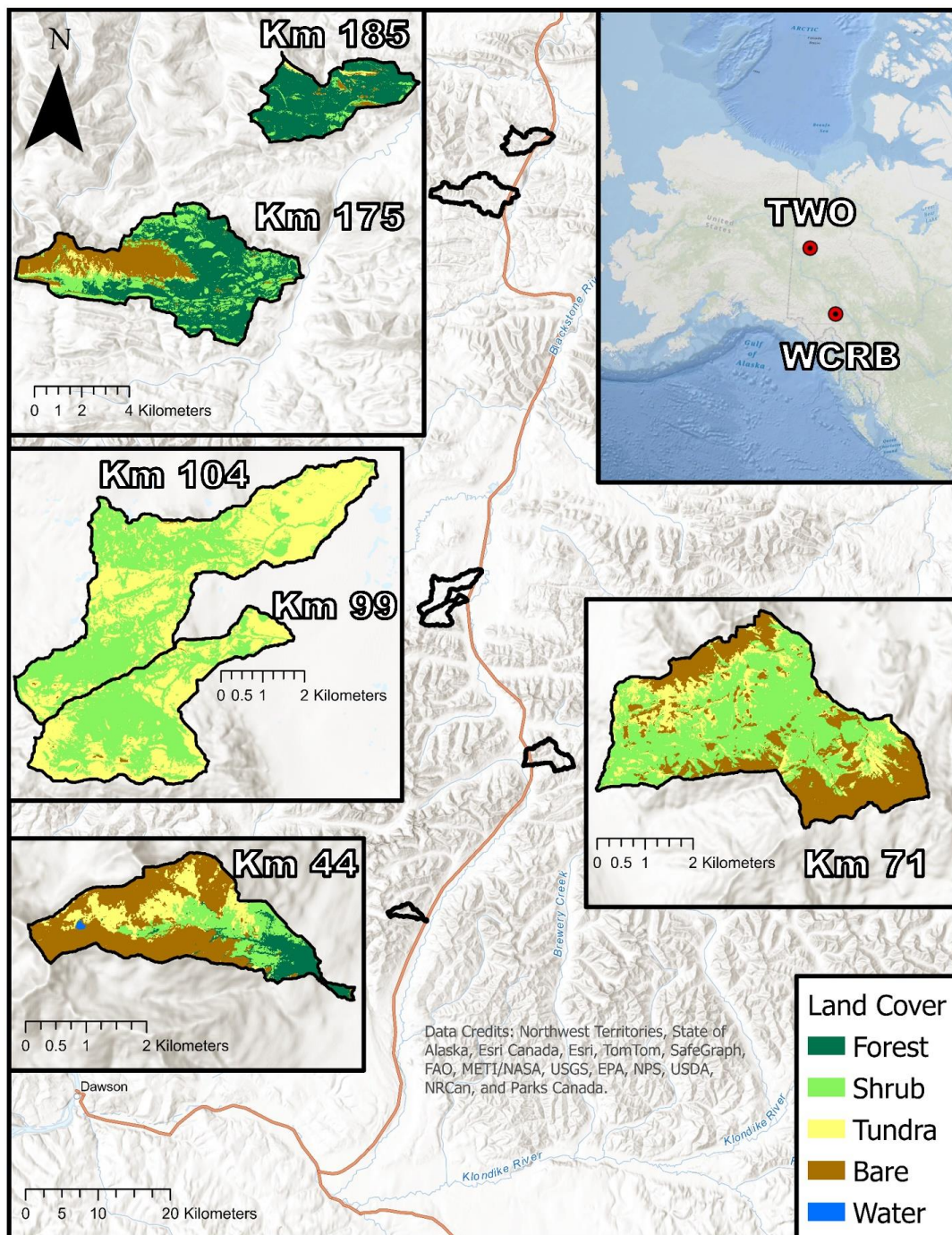
163

164 Bedrock geology across TWO is diverse (Colpron, 2022). Km 44 is primarily underlain by thick-bedded
165 quartz arenite. Km 71 is primarily underlain by two geological units; the first is described as dark grey
166 argillite, slate, and phyllite, commonly graphitic and the second is described as black graptolitic shale
167 and black chert. Km 99 and 104 are underlain by black shale and chert, dolomitic siltstone, calcareous
168 shale, and buff platy limestone in the low-lying areas. The uplands of the basins are underlain by
169 interbedded maroon and apple-green slate, siltstone, and sandstone. Km 175 and 185 are primarily
170 underlain by grey and buff-weathering dolostone, limestone, black graptolitic shale, minor chert shale,
171 siltstone, and sandstone (Colpron, 2022).

172



173 Figure 1. Study area map of Wolf Creek Research Basin (Wolf Creek Outlet, WCO) and its subcatchments
174 (Granger Creek, GC, Buckbrush Creek, BB, and Coal Lake, CL)





176 Figure 2. Study area map of all Tombstone Waters Observatory (TWO) catchments. Insets show land
177 cover for each catchment.

178 2.2. Catchment characterization

179 All TWO catchments were delineated using the 2 m resolution ArcticDEM product, whereas WCRB
180 catchments were delineated using a 1-m DEM generated from a 2018 LiDAR scan. All topographic
181 parameters including aspect, slope, and mean elevation were calculated in SAGA GIS. Land cover was
182 determined through a supervised classification using a resampled DEM and Sentinel-2 multiband
183 imagery via the *RStoolbox* package in R (Leutner et al., 2023). Catchment characteristics are reported in
184 Table 1.

185 Table 1. Table of catchment characteristics for WCRB and TWO catchments.

Site	Area (Km ²)	Forest (%)	Shrub (%)	Tundra (%)	Bare (%)	Water (%)	Elevation (m.a.s.l)	Slope (deg)	Permafrost
Km 44	5.5	12.4	17.2	18.5	51.6	0.3	1413.9	26.7	Sporadic
Km 71	16.5	0.0	48.4	17.7	33.9	0.00	1429.5	25.1	Continuous
Km 99	11	0.0	50.7	48.3	0.9	0.1	1401.5	10.9	Continuous
Km 104	17.8	0.0	50	49.6	0.4	0	1251.2	6.8	Continuous
Km 175	35.9	48.2	25.6	3.4	22.8	0	1003.2	19.2	Discontinuous
Km 185	14.7	84.3	8.8	3.5	3.4	0	916.2	18.9	Continuous
BB	5.4	0	29.7	23	46.8	0	1678	17.5	Discontinuous
GC	7.3	0	40.5	31.5	26.6	0	1618.7	11.1	Discontinuous
CL	67.8	0.4	55.4	29.7	11.8	2.7	1464	15.4	Sporadic
WCO	169.4	25.3	46	19.3	7.5	1.9	1303.7	12.3	Sporadic

186

187 2.3. Stream chemistry

188 Grab samples for major ions and DOC were collected across flow states (in spring and summer) at all
189 sites over multiple years. Grab samples were collected from 2017 to 2022 for WCO and GC. We collected
190 samples from 2018 to 2022 for Km 99, CL, and BB. Only samples from 2021 and 2022 were collected for
191 Km 104. Lastly, samples were collected from 2019 to 2022 for all other sites. Major ions and DOC
192 samples were filtered through a 0.45 µm syringe filter and collected in 60 mL HDPE bottle (DOC samples
193 stored in a brown HDPE bottle). After collection, samples were kept cool and dark in the field via



194 icepacks and immediately refrigerated at 4 °C for storage. Specific conductance (SpC) was determined in
195 the field using a multiparameter sonde (YSI proPlus or proDSS). Only one year of samples were included
196 for Km 104. The number of observations varied among sites and ranged from 24 (SpC at CL) to 92 (major
197 ions at WCO). The number of samples for each solute and site can be found in Table S1.

198 Major ions analysis was conducted via ion chromatography (DIONEX ICS 6000, IonPac AS18 and CS12A
199 analytical columns) at the University of Waterloo Biogeochemistry Lab. All DOC analysis was conducted
200 on Shimadzu TOC-5000A Total Organic Carbon Analyzer by the Biogeochemical Analytical Service
201 Laboratory in the University of Alberta. The US Environmental Protection Agency Test Method 415.1 was
202 followed (Environmental Protection Agency (EPA), 1974). Out of all the ions measured, only Ca, Mg, and
203 Sulphate had concentrations consistently over the detection limit, and were the only major ions
204 considered for analysis. Continuous SpC was measured using HOBO Conductivity loggers. The loggers
205 were calibrated in post using the YSI ProDSS handheld multiparameter sonde. If samples had
206 concentrations below the detection limit, a value of half of the detection limit was assigned to the
207 sample.

208 **2.4.Runoff**

209 All ten catchments were instrumented with Solinst levelloggers to determine continuous volumetric flow
210 rate via stage-discharge relationships. Flow measurements were generally conducted in association with
211 a chemistry grab sample. If samples were collected without a flow measurement, we used discharge
212 determined from stage-discharge relationship and continuous level loggers. The majority of the
213 catchments had very low or zero discharge over the winter. The study sites often had channel ice which
214 made winter stage-discharge relationships highly uncertain and as such there was limited winter data
215 available. Flow data was generally available during spring freshet with the exception BB, where spring
216 flow data is limited due to logistical access constraints during the snowmelt period. Discharge data is
217 available from 2017-2022 at the WCRB sites, and from 2019-2022 at the TWO sites. Km 104 was
218 instrumented late 2021 and only had data from 2022.

219 **2.5.Generalized Additive Models**

220 Generalized Additive Models (GAMs) extend traditional linear models by allowing the addition of terms
221 that are a sum of smooth functions (Hastie and Tibshirani, 1986). The additional terms can be linear or
222 non-linear spline terms, and the flexibility of the spline terms can be set by the user to prevent



223 overfitting. In this study, we use GAMs to extend the traditional concentration-discharge models by
224 adding day of year as a spline term to the linear CQ model.

$$225 \quad \log(C) = b * \log(Q) + \log(a) + sDOY \quad (1)$$

226 Where DOY is the day of year of the sample (sDOY indicates a spline fit), Q is discharge, C is the
227 concentration of the solute, and b and a are constant coefficients. This equation can also be expressed:

$$228 \quad C = e^{s(DOY)} a Q^b \quad (2)$$

229 GAMs provide the effective degrees of freedom (edf) for the spline term and provide p-values for both
230 the sDOY term and the log-log slope. The standard error for the spline term can also be extracted from
231 the model, however the standard error is not constant. In this case, standard error for the sDOY term
232 may be higher during freshet than mid-summer due to high interannual difference in discharge. The
233 mean standard error for sDOY can be used to determine the average uncertainty in the seasonality of a
234 model. The range of the sDOY fit can be used to quantify the degree of seasonality in a CQ model, where
235 a greater sDOY range means greater relative change in concentrations across seasons at a constant
236 discharge.

237 We fit a GAMs model for all five reported solutes across all ten sites, where each model was fit using the
238 restricted maximum likelihood (REML) estimation. The mgcv package in R was used for all analyses
239 involving GAMs (Wood, 2023). GAMs provide a partial effect plot, which is the measure of the influence
240 a particular term has on the model. We extracted the *b* term, the R^2 value, sDOY range, p-values for both
241 the *b* term and the sDOY term, and the mean sDOY standard deviation from each model.

242 The presence of heterogeneity in sources within the catchment and changes in connection to these
243 sources due to ground thaw will be indicated by statistical significance in both the log-log slope and the
244 sDOY term. A non-significant log-log slope with significant seasonality suggests other processes (i.e. in
245 stream biogeochemical processes) are driving seasonality. A greater sDOY range in catchments with
246 greater permafrost extent will support the second hypothesis, suggesting a greater relative change in
247 concentrations due to ground thaw.



248 **2.6. Coefficient of Variation Ratios**

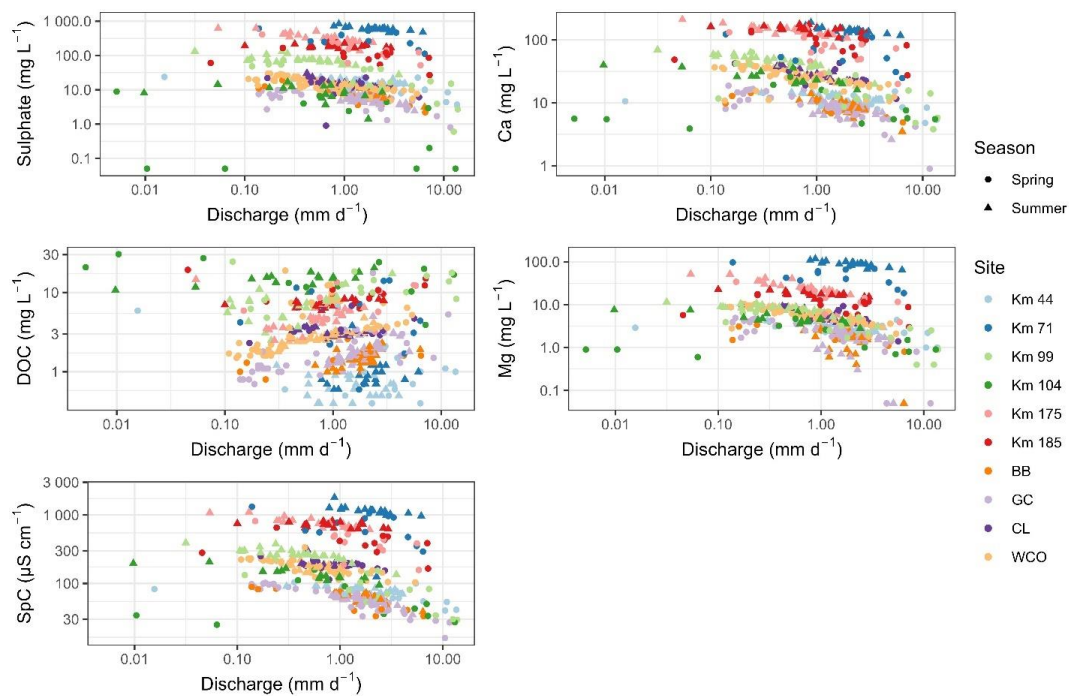
249 Ratios of the coefficient of variation of logged concentrations (CV_C) and of logged runoff (CV_Q) were used
250 to quantify chemodynamic behaviour for solutes even when there was no directionality with runoff
251 (Musolff et al., 2015; Thompson et al., 2011). We calculated $CV_C:CV_Q$ for all solutes at all sites and the CV
252 ratios were plotted against the log-log term as shown in Equation 1 and 2. CV ratios are a useful tool to
253 broadly compare chemodynamic behaviour across catchments and solutes, particularly in situations
254 where multiple distinct drivers influence stream chemistry.

255 3. Results

256 **3.1. Discharge and Concentrations Across Basins**

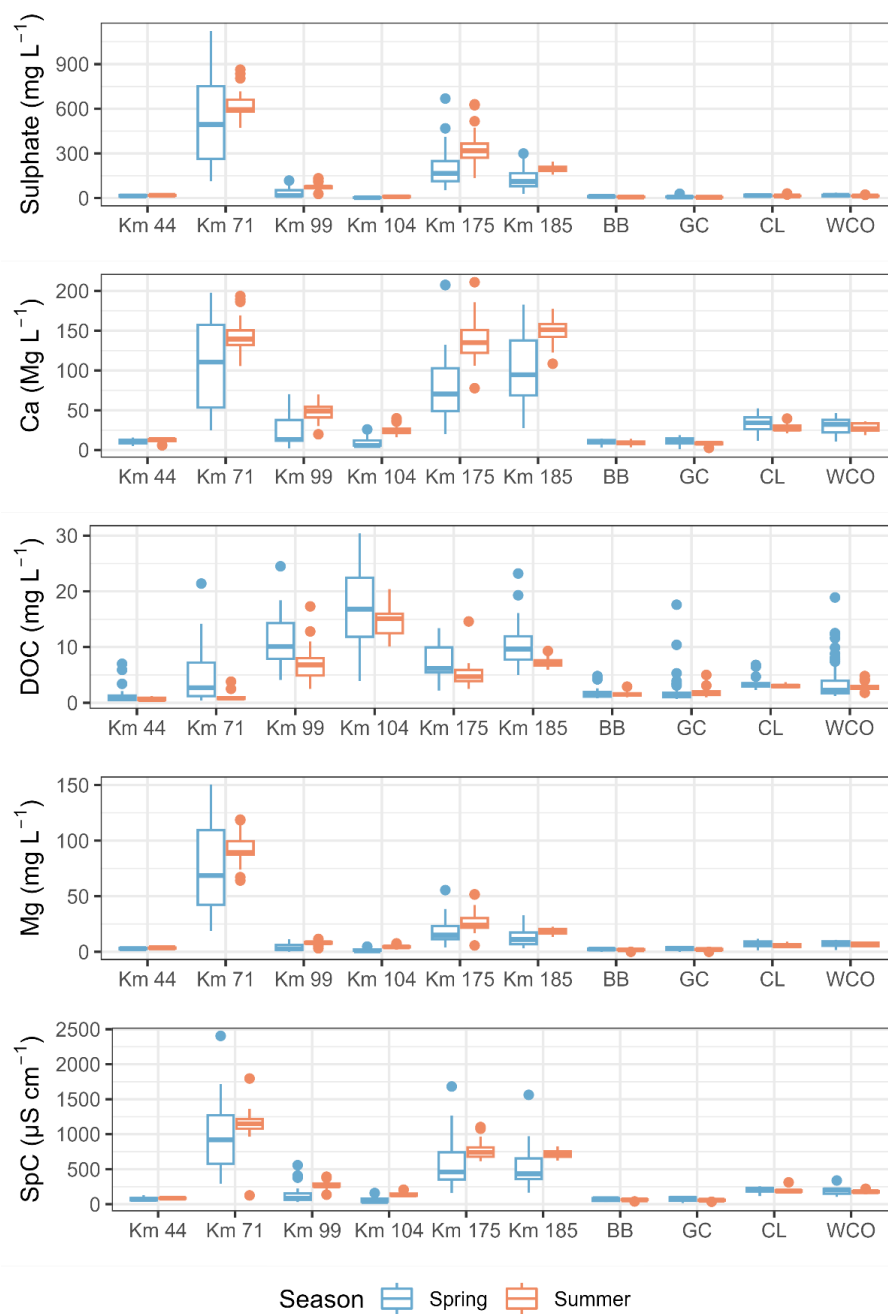
257 We determined the median of specific discharge estimates of grab samples from each site as opposed to
258 the mean to account for missed sampling at extreme low and high flows at certain sites. Median specific
259 discharge was the greatest at Km 44 and Km 71 (2.2 mm d^{-1} and 2.03 mm d^{-1} respectively). The lowest
260 median specific discharge occurred at Km 99, WCO, and Km 104 (0.57 mm d^{-1} , 0.64 mm d^{-1} , and 0.65 mm
261 d^{-1} respectively). Of note, Km 44 and 71 were adjacent sites and had strongest topographical gradients
262 (most mountainous; Table 1), whereas Km 99 and Km 104 were adjacent and had the weakest
263 topographical gradients (least mountainous).

264 Solute concentrations were generally lower at all WCRB sites compared to TWO sites (Figure 3). Km 71
265 typically had the highest concentrations of major ions, particularly Mg (median concentration of 87.6 mg
266 L^{-1}). Km 175 and Km 185 (underlain by discontinuous and continuous permafrost respectively) also had
267 relatively high concentrations of major ions across both seasons (Figure 4). Km 104 and Km 99 had the
268 highest mean concentrations of DOC, with median concentrations of 15.2 mg L^{-1} and 8 mg L^{-1}
269 respectively. In contrast, the lowest DOC concentrations generally occurred at the WCRB sites and Km
270 44. Concentrations in spring were typically more variable than late season across sites, likely due to high
271 variability in discharge (Figure 2).



272

273 Figure 3. Solute concentrations plotted against flow for all sites. Winter samples were lumped in with
274 spring.





276 Figure 4. Boxplots depicting log solute concentrations for Spring and Summer for all catchments. Winter
277 values were grouped into spring and grab samples where flow was not available are also included in the
278 boxplots. Samples taken on a DOY between 130 and 280 were classified as summer samples.

279 3.2. GAMs

280 3.2.1. Seasonality

281 Results from the GAMs indicate that not all sites showed significant seasonality for all solutes (Figure 5),
282 which was defined by a p-value lower than 0.05 for the sDOY term. The degree of seasonality, defined as
283 sDOY range, is reported in the SI (Table S1). Larger sDOY range indicates greater seasonal change in
284 concentrations after accounting for discharge. In general, sDOY increased as the season progressed post
285 freshet for major ions but decreased for DOC (Figure 5). Thus, DOC concentrations decreased over time,
286 but major ion concentrations increased at most sites after accounting for changes in flow. The WCRB
287 sites exhibited less seasonality (lower sDOY range) for major ions than the TWO sites, which typically
288 have more permafrost than WCRB sites. Model performance was generally lower for DOC than other
289 solutes, particularly for CL (a large lake dominant subcatchment of WCRB underlain with sporadic
290 permafrost), Km 175, and Km 104, which had an R^2 less than 0.2. The models exhibited poor
291 performance ($R^2 < 0.25$) in predicting Sulphate and SpC in CL, as well as in predicting Mg in BB (an alpine
292 headwater subcatchment of WCRB; Figure 6). It is important to emphasize that BB had limited
293 winter/spring samples, which may lead to lower sDOY range.

294 DOC had significant seasonality (sDOY p-value < 0.05) at all sites except for CL, Km 104, and Km 175
295 (Figure 5). Among the sites with significant seasonality, BB and Km 99 had the least pronounced
296 seasonality for DOC, characterized by sDOY ranges of 0.52 and 0.76 respectively. Conversely, Km 44 and
297 Km 71, the two catchments with the strongest topographical gradients, had the most pronounced
298 seasonality, with sDOY ranges of 1.60 and 2.35 respectively. In general, the standard error for sDOY was
299 notably higher for DOC compared to other solutes, particularly at sites exhibiting wider sDOY ranges.

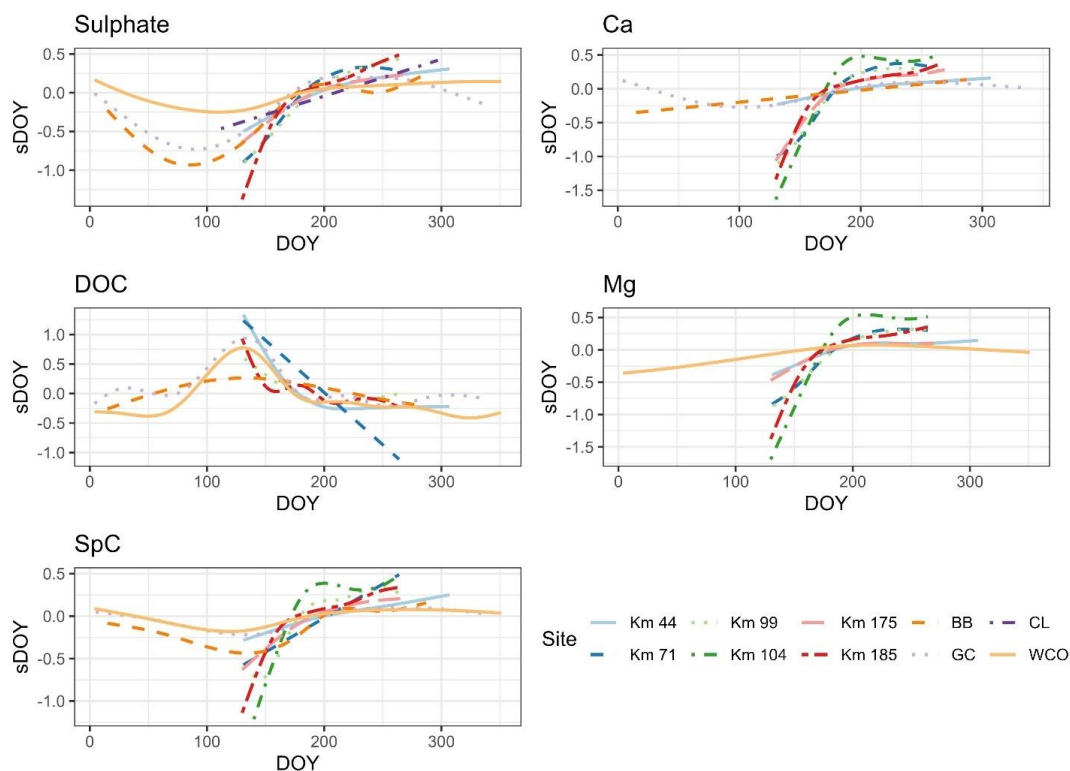
300 Sulphate exhibited significant seasonality at across all sites. The site with the least pronounced
301 seasonality was WCO (the largest catchment in our study underlain with sporadic permafrost), with an
302 sDOY range of 0.42. In contrast, Km 104 (continuous permafrost) had the greatest seasonality (sDOY
303 range: 4.1) coupled with a relatively large mean standard error (0.43) for the sDOY term. Several spring
304 samples had Sulphate concentrations below the detection limit, potentially explaining the high



305 uncertainty at Km 104 compared with other catchments. Km 185 (continuous permafrost) had the
306 second highest sDOY range (1.87) for sulphate with a lower mean standard error (0.1).

307 The GAMs seasonality results were similar for Ca, Mg, and SpC. WCO and CL, the two largest catchments,
308 were the only sites that did not have a significant sDOY term for Ca (p-values: 0.051 and 0.16,
309 respectively). Among the WCRB sites, Mg only exhibited significant seasonality at WCO. Among the TWO
310 sites, Km 175 was the only site to not exhibit significant seasonality for Mg. SpC had significant
311 seasonality for all sites except for CL (p-value: 0.37). Km 104 and Km 185 had the greatest seasonality for
312 Ca, Mg, and SpC. For Ca, sDOY ranges were 2.14 and 1.41 for Km 104 and 185 respectively. For Mg, Km
313 104 and Km 185 had sDOY ranges of 2.23 and 1.73 respectively. Km 104 and Km 185 had sDOY ranges of
314 1.69 and 1.48 respectively for SpC.

315 The lowest significant seasonality for Ca, Mg, and SpC all generally occurred at WCRB sites, which have
316 less permafrost than the TWO sites. GC and Km 44 had the weakest the weakest significant seasonality
317 for Ca, with sDOY ranges of 0.39 and 0.4 respectively, while WCO had the lowest significant seasonality
318 for Mg (sDOY range: 0.43). In contrast, Granger and WCO had the lowest significant seasonality for SpC
319 with sDOY ranges of 0.32 and 0.28 respectively. Complete GAMs results are reported in the SI.



320

321 Figure 5. sDOY from GAMs for all solutes and sites where the sDOY was significant (p -value < 0.05) and
322 mean SE was less than 0.4.

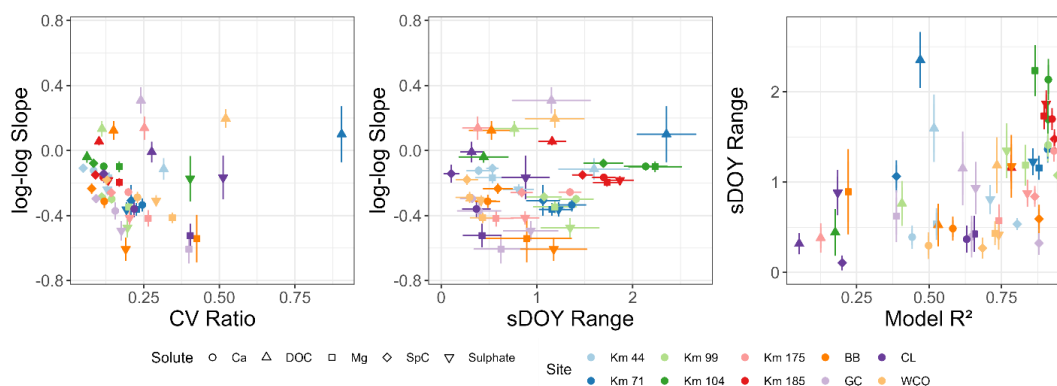
323 3.2.2. CV ratios and log-log slopes

324 Log-log slopes from the GAMs were generally negative for major ions, and positive or close to zero for
325 DOC (Figure 6). Slopes close to zero indicate spatial and vertical homogeneity of solute source within the
326 catchment, or dominance of in-stream/near-stream biogeochemical processes. The standard errors of
327 the log-log slopes were typically higher for sulphate and DOC than any other solute among sites. BB and
328 GC (alpine headwater subcatchments of WCRB) for Mg had the strongest negative slopes, approaching -
329 0.6. For DOC, WCO (outlet of WCRB) and Granger had the strongest positive log-log slopes (0.20 and 0.31
330 respectively). Km 71 (strong topographical gradient), CL (lake influenced subcatchment of WCRB), and
331 Km 104 (flat with continuous permafrost) had negative or near zero log-log slopes. All other sites had
332 weak but positive log-log slopes for DOC close to 0.1. CV ratios for all major ions were lower than 0.7 at
333 all sites, however the majority of sites had CV ratios of less than 0.3. Km 71 had the highest CV ratio for



334 DOC followed by WCO. Km 104 and CL had relatively high CV ratios for Sulphate but also had large
335 standard errors in log-log slopes. Km 104 and Km 44 (strong topographical gradient) had some of the
336 lowest CV ratios for ions along with log-log slopes close to zero, indicative of chemostatic behaviour. A
337 similar pattern can be observed for DOC for Km 104 and Km 185.

338



339

340 Figure 6. CV ratio plotted against log-log slopes from GAM models (top). Gam R² plotted against sDOY
341 range (bottom). Error bars indicate standard error of sDOY range (mean sDOY SE * $\sqrt{2}$) and the standard
342 error of the log-log slope from GAMs models. The sDOY range for Sulphate for Km 104 was large and was
343 not included in these plots for visualization purposes. Several samples were below the detection limit for
344 Sulphate at Km 104 potentially leading to high uncertainty in the model.

345 4. Discussion

346 In permafrost influenced catchments, solute concentrations are typically highly seasonal (Carey, 2003;
347 Koch et al., 2021; MacLean et al., 1999; Shatilla and Carey, 2019; Shogren et al., 2021; Townsend-Small et
348 al., 2011). Concentrations of DOC generally decrease, and concentrations of weathering derived ions
349 generally increase over the course of the spring to fall transition. Seasonal active layer dynamics,
350 depleting solute stores, and seasonality in discharge have been used to explain these patterns previously
351 (Carey, 2003; Shatilla and Carey, 2019). However, little work has been done to resolve the relative
352 influence of these drivers of variability. Here we provide insights on the mechanisms of solute export in
353 permafrost underlain catchments by assessing changes in CQ relationships.



354 Results largely confirm our first hypothesis, which states that after accounting for the seasonality in
355 discharge, concentrations for DOC would decrease and the concentrations for major ions would increase
356 post freshet due to seasonal ground thaw. However, our results also suggest that depletion of soil
357 organic matter during spring, not ground thaw, is the primary driver for seasonality in DOC
358 concentrations.

359 Our second hypothesis states that greater permafrost extent would lead to greater seasonality for major
360 ions and DOC. Although we found evidence to support this hypothesis for major ions, our results indicate
361 that permafrost is less important than other catchment characteristics (i.e. topographical gradients)
362 when considering seasonality of DOC.

363 **4.1. Seasonal drivers for DOC and major ions**

364 **4.1.1. Spatial/vertical heterogeneity in soil chemistry is evident in most catchments**

365 Log-log C-Q slopes were predominantly negative (dilution) for all major ions and positive (flushing) or
366 with no significant slope for DOC. This corresponds to work of others who reported log-log slopes as
367 typically positive for DOC (MacLean et al., 1999; Skierszkan et al., 2024) and negative for major ions
368 (MacLean et al., 1999; Shatilla et al., 2023) in permafrost underlain catchments. The negative log-log
369 slopes for major ions indicates the presence of greater mineral rich soils at depth. Log-log CQ slopes for
370 major ions were closest to zero for Km 104 (a relatively flat catchment with uniform catchment
371 characteristics), indicating high homogeneity in terms of the spatial and vertical distribution of solute
372 sources within the catchment.

373 A near zero log-log slope suggests that mobile organic carbon (OC) may be homogeneous
374 vertically/spatially, or in-stream/near-stream biogeochemical processes drive variability in DOC
375 concentrations (Creed et al., 2015; Zhi and Li, 2020). Although many catchments had significant positive
376 log-log slopes for DOC; CL, Km 44, Km 71, Km 104, and Km 175 all had non-significant log-log DOC slopes.
377 Km 104 has near zero log-log slopes with a very low CV ratio. The low log-log slopes likely reflect the
378 largely homogeneous vertical/spatial soil profile due to thick organic soils and relatively thin active layer
379 (~40 cm), and weak topographical gradients. Additionally, the stream is slow moving and instream
380 processes may be more important in this catchment than the other TWO catchments. CL is the second
381 largest catchment in this study with a ~1 km² lake just above the sampling outlet. The non-significant log-
382 log slope along with high CV ratio at CL indicate the dominance of in-stream/surface water processes (i.e.



383 photosynthesis, respiration, photo-oxidation), as high heterogeneity of catchment characteristics in
384 WCRB rule out homogeneity in vertical and spatial soil characteristics as a potential driver for low log-log
385 slopes. Both Km 104 and CL had insignificant sDOY terms and near zero log-log slopes, indicating the lack
386 of seasonality in DOC concentrations.

387 Despite the near zero log-log slopes, the high seasonality of Km 44 and Km 71 for DOC (Section 3.2)
388 suggests seasonal processes other than discharge and active layer thaw are primary drivers of variability
389 of DOC in these catchments. Km 44 and Km 71 have strong topographic gradients, a thin organic layer
390 along with a high proportion of bare ground; particularly upslope of riparian areas. This result suggests
391 that as the source area expands during high flows, water with low DOC concentrations from upslope
392 rocky areas (which do not have a defined organic layer) move quickly through the organic layer near
393 riparian areas (limiting contact time) due to the steep gradients and dilute the stream DOC signal.

394 **4.1.2. Seasonal depletion of soil stores is important for DOC export**

395 Our analysis suggests that flushing of organic soils during freshet is likely the primary driver for seasonal
396 declines in DOC, yet active layer thaw may be secondary driver depending on the spatial/vertical
397 distribution of organic matter concentrations in soil. At most sites, high seasonality for DOC (as indicated
398 by the sDOY range) along with nonsignificant log-log slopes indicates changing flow paths due to active
399 layer thaw is likely not the primary driver in the seasonality of DOC concentrations (Figure 6). In this
400 scenario, seasonality in DOC concentrations would be driven primarily via flushing of organic soils during
401 freshet. The seasonality term in GAMs accounts for changes in flow, and the presence of non-significant
402 log-log slopes indicate a lack of vertical heterogeneity in soil OC concentrations or dominance of in/near-
403 stream processes. Thus, seasonality in CQ relationships for DOC in catchments where log-log slopes are
404 near zero, must be driven by processes other than changing flow paths due to active layer thaw or
405 discharge. Previous work in snow dominated mountains has shown the flushing of organic matter in soils
406 during freshet can reduce the soil reservoir of DOC (Boyer et al., 1997; Hornberger et al., 1994). For
407 example, Boyer et al. (1997) attributed declines in DOC as melt progressed to source depletion in the
408 upper soil horizons in a mountain headwater catchment in Colorado, USA. Certain sites (GC, WCO, BB,
409 Km 99, and Km 175) did have positive log-log slopes for DOC, suggesting that depletion of DOC stores
410 and thawing active layer may have a combined effect in controlling DOC concentrations. The strong
411 decline of the sDOY term during freshet at several sites indicates (Figure 5) that flushing of DOM in soils
412 during freshet rapidly deplete finite labile OC stores within catchment soils as observed elsewhere



413 (Boyer et al., 1997; Hornberger et al., 1994). Previous work at GC, attributed a strong hysteresis of DOC
414 concentrations during freshet and summer events to both a rapid decline in organic matter and greater
415 emphasis on deeper flow pathways (Carey, 2003; Shatilla and Carey, 2019). Townsend-Small et al. (2011)
416 compared DOC concentrations at the same discharge level in the upper Kuparuk River in Alaska and saw
417 a decrease in DOC concentrations over time, suggesting seasonality is at least partially driven by active
418 layer thaw and/or depleting solute stores. Skierszkan et al. (2024) used a mixing model and found
419 seasonality in DOC concentrations to primarily be driven by changing flow paths in the Dawson range,
420 Yukon, Canada, which contrasts with our findings. This discrepancy is potentially a result of strong
421 heterogeneity in spatial and vertical soil OC concentrations in the Dawson range, and greater presence of
422 organic carbon in soils.

423 **4.1.3. Seasonal active layer freeze-thaw is important for major ion export**

424 Our study largely agrees with others in permafrost environments that attributed the seasonality of major
425 ions to seasonal active layer thaw. Similar to other studies, we found CQ relationships are variable
426 among seasons for major ions in permafrost underlain catchments (MacLean et al., 1999; Shatilla et al.,
427 2023). Non-zero log-log slopes indicate presence of heterogeneity in soil chemistry. Significant sDOY
428 terms indicate seasonal changes in ion concentration after accounting for variability in discharge. The
429 negative log-log slopes and strong seasonality at multiple sites for multiple major ions suggest that
430 activation of different flow paths from seasonal active layer thaw along with discharge influence export
431 in these regions. Thawing of the active layer leads to greater flow from the deeper mineral rich soil
432 horizons and bedrock and consequently higher ion concentrations. GAM results for major ions indicate
433 seasonal increases in solute concentrations, suggesting the seasonality in CQ patterns is not primarily
434 driven by depletion of ion stores (Figure 5). Shatilla et al. (2023) attributed ground thaw and increasing
435 connectivity of deep groundwater to seasonal increases in solute concentrations in GC. (Lehn et al.,
436 2017) attributed a seasonal increase of major ion concentrations in Alaskan watersheds to seasonally
437 thawing active layer and cryoconcentration in soils during later fall and winter of the previous years. Our
438 results are generally in agreement with these findings, although we did not have the data to assess the
439 influence of cryoconcentration in soils. Km 104 had significant but relatively low log-log slopes, with the
440 highest seasonality. This suggests that other drivers (aside from discharge and active layer thaw) may
441 play an important role in seasonal ion concentrations in this site. Km 104 and Km 99 were found to have
442 highly seasonal transit time distributions, where the fraction of young water is much lower in the
443 summer than in the spring (unpublished data). Greater transit times in the summer can lead to greater



444 contact time between water and mineral systems (Benettin et al., 2015), potentially driving seasonality
445 in this system. However, calculating transit times requires estimates of input tracer concentrations which
446 was difficult to do for many of our study catchments, particularly during snowmelt.

447 **4.2. Catchment characteristics drive seasonality**

448 **4.2.1 Stronger topographical gradients lead to greater DOC seasonality**

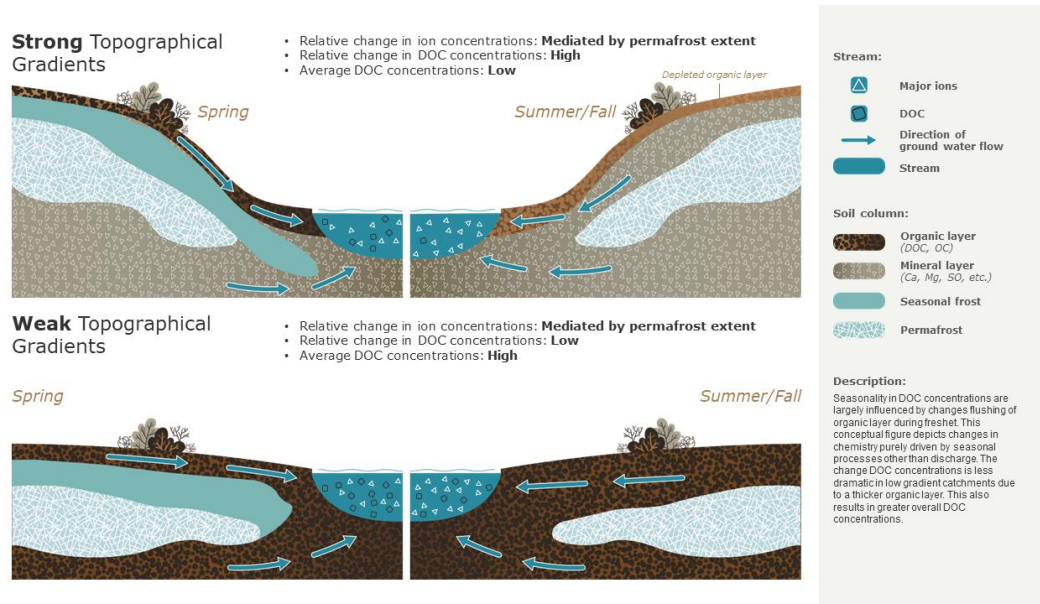
449 Although permafrost extent has a strong influence on DOC export (Frey and McClelland, 2009; MacLean
450 et al., 1999; Petrone et al., 2006), greater permafrost extent did not necessarily lead to greater
451 seasonality (sDOY range) in CQ relationships for DOC. For example, DOC was highly seasonal in WCO
452 (sporadic permafrost) but had relatively low seasonality for Km 99 (continuous permafrost). Although
453 DOC concentrations were generally higher in the TWO sites, they did not necessarily exhibit a greater
454 relative change in concentrations than the sites in WCRB, which generally have a lower permafrost
455 extent than the TWO sites. Our results are in contrast to MacLean et al. (1999) and Petrone et al. (2006)
456 who observed stronger seasonality for DOC/DOM in catchments with greater permafrost extent.
457 MacLean et al. (1999) reported stronger CQ relationships and greater model performance for DOC in a
458 high permafrost catchment compared to the low permafrost catchment in central Alaska during the
459 summer. However, CQ relationships were similar between the catchments during snowmelt. The authors
460 attributed this to a lower variability in discharge during the summer for the low permafrost catchment.
461 Petrone *et al.* (2006) observed larger increases of DOC export in catchments with greater permafrost
462 extent. However, Petrone *et al.* (2006) did not assess the relative changes in DOC export or seasonality in
463 discharge, where connectivity to DOC changes with changing catchment wetness.

464 In our study sites, catchment characteristics related to slope and specific discharge were more important
465 for DOC seasonality than permafrost extent. For example, the two most mountainous sites (Km 44 and
466 Km 71) had the highest seasonality for DOC, indicating the greatest relative seasonal changes in
467 concentrations after accounting for discharge. Both Km 44 and Km 71 had high specific discharge, strong
468 topographical gradients, and the lowest average concentrations for DOC, supporting the idea that
469 organic matter stores were limited. Non-significant log-log slopes imply that nearly all the seasonality at
470 these sites was due to the depletion of solute stores and not due to active layer thaw as conceptually
471 outlined in Fig 7. Although other seasonal processes (water age, stream temperature, etc.) may be
472 important, flushing of soil OC has been observed as an important mechanism in multiple mountain
473 catchments (Boyer et al., 1997; Shatilla and Carey, 2019). The limited DOC supply and rapid flushing due



474 to high flows presumably led to a more rapid depletion in DOC stores in these catchments. Conversely,
475 Km 99 and Km 104 had high average DOC concentrations and high permafrost extent yet exhibited lower
476 seasonality than Km 71 and Km 44. Additionally, the CV ratio at Km 104 was also very low, indicating DOC
477 was chemostatic. Km 99 and Km 104 had much weaker topographical gradients and specific discharge
478 relative to other sites, potentially leading to limited flushing of soils (low specific discharge), which may
479 have played an important role in the weak seasonality of DOC. One caveat is that Km 104 had a very low
480 R^2 value (<0.2) for DOC and did not have significant seasonality or log-log slopes, potentially due to the
481 lack of multi-year sampling. Km 99 is similar to Km 104, but had a significant positive log-log slope for
482 DOC. Unlike Km 104, Km 99 is not entirely overlain with peat in the active layer as mineral soils are
483 present in the headwaters. The significant seasonality in Km 99 may be driven by thawing of the active
484 layer, leading to deactivation of shallow DOC rich flow paths, or due to flushing of organic layer during
485 freshet. We cannot disentangle the influence of depletion of solute stores and thawing of the active
486 layer on seasonality of DOC in catchments that do have significant log-log slopes. It is likely that in these
487 catchments, both flushing of organic soils and active layer thaw drive seasonality in DOC concentrations.

488 The presence of a lake near the outlet of CL can lead to dampening of the terrestrial DOC signal and may
489 be dominated by in-lake biogeochemical processes. This may explain the lack of significance in the sDOY
490 term in CL. Low seasonality in BB relative to GC is likely a function of limited sampling during freshet at
491 BB. Seasonality was also low in Km 175, likely due to high median Fe concentrations (1.8 mg L^{-1}) in the
492 stream (unpublished data), which may lead to the dominance of instream processes in Km 175 as Fe
493 interacts strongly with DOM (Gu et al., 1994; McKnight and Duren, 2004)(Gu et al., 1994; McKnight and
494 Duren, 2004).



495

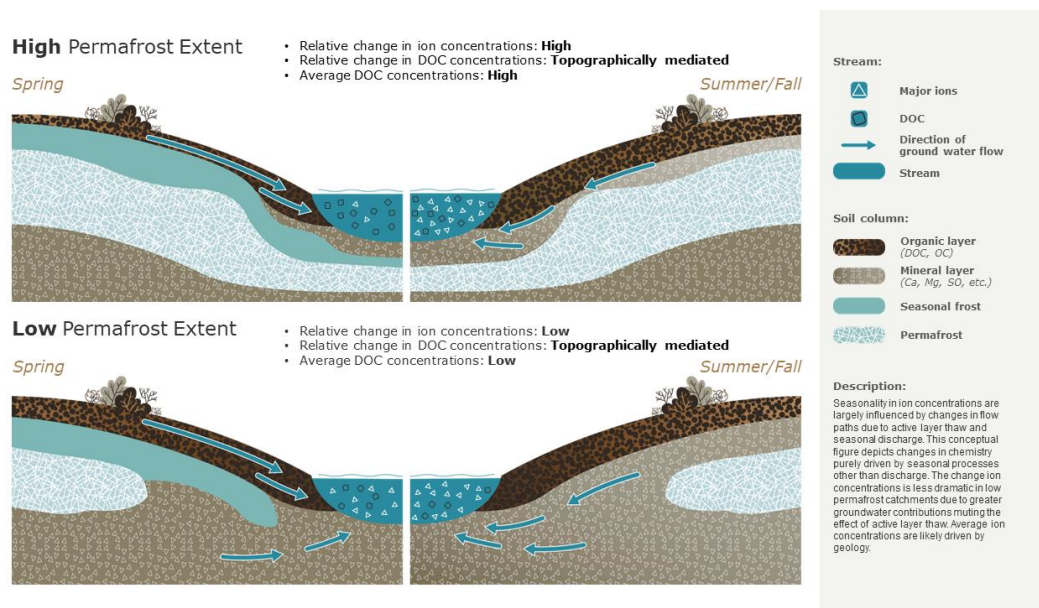
496 Figure 7. Conceptual diagram depicting the influence of topographical gradients on the relative seasonal
497 change in DOC concentrations and the mean concentration of DOC after accounting for seasonal
498 discharge.

499 4.2.2. Permafrost extent is important for major ion seasonality

500 Unlike DOC, permafrost extent and winter groundwater contributions do influence the seasonality of
501 major ions, although the overall export is likely influenced by surficial geology. In general, catchments in
502 WCRB had lower seasonality than TWO catchments for major ions. Km 44 and Km 175 were the only
503 exception to this, as these sites generally had low seasonality for major ions. This may be explained by
504 significant surface-groundwater connection throughout the ice-free season as neither of these
505 catchments are underlain with continuous permafrost as outlined conceptually in Fig 8. Our results are
506 similar to Webster et al. (2022) who observed seasonal increases in NO₃ in Alaska, which the authors
507 attributed to thawing active layer in a high permafrost extent catchment but not in low permafrost
508 catchments. The authors argued that dominance of groundwater was responsible for the lack of a
509 seasonal trend in the low permafrost catchments. This supports our hypothesis for major ions, where
510 the presence of deep groundwater contributions in low-permafrost catchments can dampen seasonality
511 of CQ relationships for major ions. However, these results should be interpreted with caution as
512 estimating permafrost extent in mountain headwater catchments is uncertain. The seasonality metrics



513 for Mg at BB have low predictive power; this is likely due to limited sampling during freshet and presence
514 of some samples that were below the detection limit.



515

516 Figure 8. Conceptual diagram depicting the influence of permafrost extent on the relative seasonal
517 change in ion concentrations and the mean concentration of DOC after accounting for seasonal
518 discharge.

519 5. Conclusion and Future Directions

520 In this study, we assessed the role of catchment characteristics, seasonal active layer thaw, and depletion
521 of solute stores in controlling solute export in permafrost underlain watersheds. We obtained new
522 insights on chemical transport through hydrochemical data collected across multiple catchments and
523 seasons, a task rarely undertaken across such a diverse range of remote, permafrost underlain
524 environments. We utilized GAMs to assess changes in connectivity to solute sources after accounting for
525 seasonally changing discharge. We largely confirmed our first hypothesis, where ion concentrations
526 increased, and DOC concentrations decreased (irrespective of seasonality in discharge) after the start of
527 freshet. However, we found evidence of differing drivers of seasonality between DOC and major ions;
528 seasonality in DOC was primarily caused by flushing of OC from soils stores during freshet, while
529 seasonality in major ions was driven by seasonal active layer thaw. For major ions, our second hypothesis



530 suggesting permafrost extent drove variability in chemical concentrations was found to be largely true.
531 However, although permafrost extent was important for the average concentrations of DOC, topography
532 was a more important driver in terms of seasonality as mountainous catchments with thin organic soils
533 and high specific discharge lead to rapid flushing of limited soil OC stores.

534 GAMs can be a useful tool to assess the influence of non-linear terms. Long term trend analysis of solute
535 concentrations is often confounded by long term trends in runoff. For example, long term increases in
536 major ion concentrations may be driven by long term decreases in runoff. Using partial effect plots in a
537 CQ framework within GAMs can allow for the assessment of long-term trends in chemistry after
538 accounting for long term trends in flow. Water transit times may be an important driver of variability of
539 stream chemistry as it can indicate contact time of water with mineral substrate. This would particularly
540 be true in permafrost environments, where transit times of water can be highly seasonal. Future work
541 should incorporate the influence of transit times on seasonality of stream chemistry in permafrost
542 catchments.

543 Our results suggest climate change induced increases in active layer thickness and greater connectivity of
544 subpermafrost, inter-permafrost, and suprapermafrost water will lead to elevated concentrations of
545 weathering derived ions, reduced concentration of DOC and a decrease in seasonality of major ions in
546 high latitude catchments. The role of permafrost extent on the seasonality of DOC concentrations
547 remains unclear. This work highlights the need for long-term stream chemistry sampling across a
548 biogeophysical range of high latitude watersheds. Greater sampling resolution could provide a means of
549 quantifying the influence of secondary drivers (i.e. stream temperature) on stream chemistry in these
550 environments. Currently, much of the literature assesses the role of catchment characteristics on solute
551 exports, but limited work has been done on the drivers of seasonality in cold regions largely due to the
552 lack of sampling in the shoulder seasons. This study is one of the few to assess the drivers of seasonality
553 of stream chemistry in permafrost underlain catchments.

554 Data Availability Statement

555 The data used in this study is available in a Zenodo repository (DOI: 10.5281/zenodo.13621953; Grewal
556 et al., 2024).



557 Author Contributions

558 AG, SKC, and EMN conceptualized the study and reviewed/edited the manuscript. AG and EMN collected
559 and curated the data. AG developed the methodology, conducted the analysis, made figures, and wrote
560 the original manuscript draft. SKC was the principal investigator and acquired funding for the project.

561 Conflict of Interest

562 The authors declare that they have no conflict of interest.

563 Special Issue Statement

564 This article is part of the special issue “Northern Hydrology in Transition”. It is not associated with a
565 conference.

566 Acknowledgments

567 We would like to thank David Barrett, Tyler de Jong, Fiona Chapman, Joseph Desmarais, Sean Leipe,
568 Lauren Bourke, Aliana Fristensky, Anna Grunsky, Andras Szeitz, and Calvin Newbery for field assistance.
569 We would like to thank Global Water Futures, and National Science and Engineering Council of Canada
570 (RGPNS-2020-06722) for providing financial support for this project. We acknowledge the continued
571 support of the Water Resources Branch, Government of Yukon, for the operation of Wolf Creek Research
572 Basin.

573 References

- 574 Benettin, P., Bailey, S. W., Campbell, J. L., Green, M. B., Rinaldo, A., Likens, G. E., McGuire, K. J., and
575 Botter, G.: Linking water age and solute dynamics in streamflow at the Hubbard Brook Experimental
576 Forest, NH, USA, *Water Resour Res*, 51, 9256–9272, <https://doi.org/10.1002/2015WR017552>, 2015.
- 577 Biagi, K. M., Ross, C. A., Oswald, C. J., Sorichetti, R. J., Thomas, J. L., and Wellen, C. C.: Novel predictors
578 related to hysteresis and baseflow improve predictions of watershed nutrient loads: An example from
579 Ontario’s lower Great Lakes basin, *Science of the Total Environment*, 826, 154023,
580 <https://doi.org/10.1016/j.scitotenv.2022.154023>, 2022.
- 581 Bonnaventure, P. P., Lewkowicz, A. G., Kremer, M., and Sawada, M. C.: A Permafrost Probability Model for
582 the Southern Yukon and Northern British Columbia, Canada, *Permafr Periglac Process*, 23, 52–68,
583 <https://doi.org/10.1002/ppp.1733>, 2012.



- 584 Boyer, E. W., Hornberger, G. M., Bencala, K. E., and McKnight, D. M.: Response characteristics of DOC
585 flushing in an alpine catchment, *Hydrol Process*, 11, 1635–1647, [https://doi.org/10.1002/\(SICI\)1099-1085\(19971015\)11:12<1635::AID-HYP494>3.0.CO;2-H](https://doi.org/10.1002/(SICI)1099-1085(19971015)11:12<1635::AID-HYP494>3.0.CO;2-H), 1997.
- 587 Carey, S. K.: Dissolved organic carbon fluxes in a discontinuous permafrost subarctic alpine catchment,
588 *Permafr Periglac Process*, 14, 161–171, <https://doi.org/10.1002/ppp.444>, 2003.
- 589 Carey, S. K. and Woo, M.: Slope runoff processes and flow generation in a subarctic, subalpine
590 catchment, *J Hydrol (Amst)*, 253, 110–129, [https://doi.org/10.1016/S0022-1694\(01\)00478-4](https://doi.org/10.1016/S0022-1694(01)00478-4), 2001.
- 591 Carey, S. K., Boucher, J. L., and Duarte, C. M.: Inferring groundwater contributions and pathways to
592 streamflow during snowmelt over multiple years in a discontinuous permafrost subarctic environment
593 (Yukon, Canada), *Hydrogeol J*, 21, 67–77, <https://doi.org/10.1007/s10040-012-0920-9>, 2013.
- 594 Cohen, J., Screen, J. A., Furtado, J. C., Barlow, M., Whittleston, D., Coumou, D., Francis, J., Dethloff, K.,
595 Entekhabi, D., Overland, J., and Jones, J.: Recent Arctic amplification and extreme mid-latitude weather,
596 *Nat Geosci*, 7, 627–637, <https://doi.org/10.1038/ngeo2234>, 2014.
- 597 Colpron, M.: The Yukon Digital Bedrock Geology compilation, in: *Yukon Exploration and Geology 2021*,
598 K.E. MacFarlane (ed.), Yukon Geological Survey, 143–159, 2022.
- 599 Creed, I. F., McKnight, D. M., Pellerin, B. A., Green, M. B., Bergamaschi, B. A., Aiken, G. R., Burns, D. A.,
600 Findlay, S. E. G., Shanley, J. B., Striegl, R. G., Aulenbach, B. T., Clow, D. W., Laudon, H., McGlynn, B. L.,
601 McGuire, K. J., Smith, R. A., and Stackpoole, S. M.: The river as a chemostat: fresh perspectives on
602 dissolved organic matter flowing down the river continuum, *Canadian Journal of Fisheries and Aquatic
603 Sciences*, 72, 1272–1285, <https://doi.org/10.1139/cjfas-2014-0400>, 2015.
- 604 Environmental Protection Agency (EPA): Method 415.1: Organic Carbon, Total (Combustion Or
605 Oxidation), 1974.
- 606 Fork, M. L., Sponseller, R. A., and Laudon, H.: Changing Source-Transport Dynamics Drive Differential
607 Browning Trends in a Boreal Stream Network, *Water Resour Res*, 56,
608 <https://doi.org/10.1029/2019WR026336>, 2020.
- 609 Frey, K. E. and McClelland, J. W.: Impacts of permafrost degradation on arctic river biogeochemistry,
610 *Hydrol Process*, 23, 169–182, <https://doi.org/10.1002/hyp.7196>, 2009.
- 611 Frey, K. E. and Smith, L. C.: Amplified carbon release from vast West Siberian peatlands by 2100, *Geophys
612 Res Lett*, 32, 1–4, <https://doi.org/10.1029/2004GL022025>, 2005.
- 613 Godsey, S. E., Kirchner, J. W., and Clow, D. W.: Concentration-discharge relationships reflect chemostatic
614 characteristics of US catchments, *Hydrol Process*, 23, 1844–1864, <https://doi.org/10.1002/hyp.7315>,
615 2009.
- 616 Grewal, A., Nicholls, E. M., and Carey, S. K.: The role of catchment characteristics, discharge, and active
617 layer thaw on seasonal stream chemistry across ten permafrost catchments (Version 1) [Data set],
618 <https://doi.org/10.5281/zenodo.13621953>, 2024.



- 619 Gu, B., Schmitt, J., Chen, Z., Liang, L., and McCarthy, J. F.: Adsorption and Desorption of Natural Organic
620 Matter on Iron Oxide: Mechanisms and Models, *Environ Sci Technol*, 28, 38–46,
621 <https://doi.org/10.1021/es00050a007>, 1994.
- 622 Hall, F. R.: Dissolved Solids-Discharge Relationships: 1. Mixing Models, *Water Resour Res*, 6, 845–850,
623 <https://doi.org/10.1029/WR006i003p00845>, 1970.
- 624 Hastie, T. and Tibshirani, R.: Generalized Additive Models, *Statistical Science*, 1, 409–435,
625 <https://doi.org/10.1214/ss/1177013604>, 1986.
- 626 Hornberger, G. M., Bencala, K. E., and McKnight, D. M.: Hydrological controls on dissolved organic carbon
627 during snowmelt in the Snake River near Montezuma, Colorado, *Biogeochemistry*, 25, 147–165,
628 <https://doi.org/10.1007/BF00024390>, 1994.
- 629 Koch, J. C., Dornblaser, M. M., and Striegl, R. G.: Storm-Scale and Seasonal Dynamics of Carbon Export
630 From a Nested Subarctic Watershed Underlain by Permafrost, *J Geophys Res Biogeosci*, 126,
631 <https://doi.org/10.1029/2021JG006268>, 2021.
- 632 Lehn, G. O., Jacobson, A. D., Douglas, T. A., McClelland, J. W., Barker, A. J., and Khosh, M. S.: Constraining
633 seasonal active layer dynamics and chemical weathering reactions occurring in North Slope Alaskan
634 watersheds with major ion and isotope ($\delta^{34}\text{S}\text{SO}_4$, $\delta^{13}\text{C}\text{DIC}$, $^{87}\text{Sr}/^{86}\text{Sr}$, $\delta^{44}/^{40}\text{Ca}$, and $\delta^{44}/^{42}\text{Ca}$)
635 measurements, *Geochim Cosmochim Acta*, 217, 399–420, <https://doi.org/10.1016/j.gca.2017.07.042>,
636 2017.
- 637 Leutner, B., Horning, N., and Schwalb-Willmann, J.: RStoolbox: Tools for Remote Sensing Data Analysis,
638 2023.
- 639 Lewkowicz, A. G. and Ednie, M.: Probability mapping of mountain permafrost using the BTS method,
640 Wolf Creek, Yukon Territory, Canada, *Permafr Periglac Process*, 15, 67–80,
641 <https://doi.org/10.1002/ppp.480>, 2004.
- 642 Li, L., Knapp, J. L. A., Lintern, A., Ng, G. H. C., Perdrial, J., Sullivan, P. L., and Zhi, W.: River water quality
643 shaped by land–river connectivity in a changing climate, *Nat Clim Chang*, 14,
644 <https://doi.org/10.1038/s41558-023-01923-x>, 2024.
- 645 MacLean, R., Oswood, M. W., Irons, J. G., and McDowell, W. H.: The effect of permafrost on stream
646 biogeochemistry: A case study of two streams in the Alaskan (U.S.A.) taiga, *Biogeochemistry*, 47, 239–
647 267, <https://doi.org/10.1007/BF00992909>, 1999.
- 648 McKenzie, J. M., Kurylyk, B. L., Walvoord, M. A., Bense, V. F., Fortier, D., Spence, C., and Grenier, C.:
649 Invited perspective: What lies beneath a changing arctic?, *Cryosphere*, 15, 479–484,
650 <https://doi.org/10.5194/tc-15-479-2021>, 2021.
- 651 McKnight, D. M. and Duren, S. M.: Biogeochemical processes controlling midday ferrous iron maxima in
652 stream waters affected by acid rock drainage, *Applied Geochemistry*, 19, 1075–1084,
653 <https://doi.org/10.1016/j.apgeochem.2004.01.007>, 2004.
- 654 McNamara, J. P., Kane, D. L., and Hinzman, L. D.: An analysis of streamflow hydrology in the Kuparuk
655 River Basin, Arctic Alaska: A nested watershed approach, *J Hydrol (Amst)*, 206, 39–57,
656 [https://doi.org/10.1016/S0022-1694\(98\)00083-3](https://doi.org/10.1016/S0022-1694(98)00083-3), 1998.



- 657 Musloff, A., Schmidt, C., Selle, B., and Fleckenstein, J. H.: Catchment controls on solute export, *Adv Water*
658 *Resour*, 86, 133–146, <https://doi.org/10.1016/j.advwatres.2015.09.026>, 2015.
- 659 Obu, J., Westermann, S., Bartsch, A., Berdnikov, N., Christiansen, H. H., Dashtseren, A., Delaloye, R.,
660 Elberling, B., Etzelmüller, B., Kholodov, A., Khomutov, A., Kääh, A., Leibman, M. O., Lewkowicz, A. G.,
661 Panda, S. K., Romanovsky, V., Way, R. G., Westergaard-Nielsen, A., Wu, T., Yamkhin, J., and Zou, D.:
662 Northern Hemisphere permafrost map based on TTOP modelling for 2000–2016 at 1 km² scale, *Earth Sci*
663 *Rev*, 193, 299–316, <https://doi.org/10.1016/j.earscirev.2019.04.023>, 2019.
- 664 Petrone, K. C., Jones, J. B., Hinzman, L. D., and Boone, R. D.: Seasonal export of carbon, nitrogen, and
665 major solutes from Alaskan catchments with discontinuous permafrost, *J Geophys Res Biogeosci*, 111,
666 n/a-n/a, <https://doi.org/10.1029/2005JG000055>, 2006.
- 667 Quinton, W. L. and Marsh, P.: A conceptual framework for runoff generation in a permafrost
668 environment, *Hydrol Process*, 13, 2563–2581, [https://doi.org/10.1002/\(SICI\)1099-1085\(199911\)13:16<2563::AID-HYP942>3.0.CO;2-D](https://doi.org/10.1002/(SICI)1099-1085(199911)13:16<2563::AID-HYP942>3.0.CO;2-D), 1999.
- 670 Ran, Y., Li, X., Cheng, G., Che, J., Aalto, J., Karjalainen, O., Hjort, J., Luoto, M., Jin, H., Obu, J., Hori, M., Yu,
671 Q., and Chang, X.: New high-resolution estimates of the permafrost thermal state and hydrothermal
672 conditions over the Northern Hemisphere, *Earth Syst Sci Data*, 14, 865–884,
673 <https://doi.org/10.5194/essd-14-865-2022>, 2022.
- 674 Rasouli, K., Pomeroy, J. W., Janowicz, J. R., Carey, S. K., and Williams, T. J.: Hydrological sensitivity of a
675 northern mountain basin to climate change, *Hydrol Process*, 28, 4191–4208,
676 <https://doi.org/10.1002/hyp.10244>, 2014.
- 677 Rasouli, K., Pomeroy, J. W., Janowicz, J. R., Williams, T. J., and Carey, S. K.: A long-term
678 hydrometeorological dataset (1993–2014) of a northern mountain basin: Wolf Creek Research Basin,
679 Yukon Territory, Canada, *Earth Syst Sci Data*, 11, 89–100, <https://doi.org/10.5194/essd-11-89-2019>,
680 2019.
- 681 Ross, C. A., Moslenko, L. L., Biagi, K. M., Oswald, C. J., Wellen, C. C., Thomas, J. L., Raby, M., and
682 Sorichetti, R. J.: Total and dissolved phosphorus losses from agricultural headwater streams during
683 extreme runoff events, *Science of the Total Environment*, 848, 157736,
684 <https://doi.org/10.1016/j.scitotenv.2022.157736>, 2022.
- 685 Shatilla, N. and Carey, S.: Assessing inter-annual and seasonal patterns of DOC and DOM quality across a
686 complex alpine watershed underlain by discontinuous permafrost in Yukon, Canada, *Hydrol Earth Syst*
687 *Sci*, 23, 3571–3591, <https://doi.org/10.5194/hess-23-3571-2019>, 2019.
- 688 Shatilla, N. J., Tang, W., and Carey, S. K.: Multi-year high-frequency sampling provides new runoff and
689 biogeochemical insights in a discontinuous permafrost watershed, *Hydrol Process*, 37,
690 <https://doi.org/10.1002/hyp.14898>, 2023.
- 691 Shogren, A. J., Zarnetske, J. P., Abbott, B. W., Iannucci, F., Medvedeff, A., Cairns, S., Duda, M. J., and
692 Bowden, W. B.: Arctic concentration–discharge relationships for dissolved organic carbon and nitrate
693 vary with landscape and season, *Limnol Oceanogr*, 66, S197–S215, <https://doi.org/10.1002/lno.11682>,
694 2021.



- 695 Skierszkan, E. K., Carey, S. K., Jackson, S. I., Fellwock, M., Fraser, C., and Lindsay, M. B. J.: Seasonal
696 controls on stream metal(loid) signatures in mountainous discontinuous permafrost, *Science of the Total*
697 *Environment*, 908, 167999, <https://doi.org/10.1016/j.scitotenv.2023.167999>, 2024.
- 698 Stewart, B., Shanley, J. B., Kirchner, J. W., Norris, D., Adler, T., Bristol, C., Harpold, A. A., Perdrial, J. N.,
699 Rizzo, D. M., Sterle, G., Underwood, K. L., Wen, H., and Li, L.: Streams as Mirrors: Reading Subsurface
700 Water Chemistry From Stream Chemistry, *Water Resour Res*, 58, 1–20,
701 <https://doi.org/10.1029/2021WR029931>, 2022.
- 702 Tank, S. E., Striegl, R. G., McClelland, J. W., and Kokelj, S. V.: Multi-decadal increases in dissolved organic
703 carbon and alkalinity flux from the Mackenzie drainage basin to the Arctic Ocean, *Environmental*
704 *Research Letters*, 11, 054015, <https://doi.org/10.1088/1748-9326/11/5/054015>, 2016.
- 705 Tank, S. E., McClelland, J. W., Spencer, R. G. M., Shiklomanov, A. I., Suslova, A., Moatar, F., Amon, R. M.
706 W., Cooper, L. W., Elias, G., Gordeev, V. V., Guay, C., Gurtovaya, T. Y., Kosmenko, L. S., Mutter, E. A.,
707 Peterson, B. J., Peucker-Ehrenbrink, B., Raymond, P. A., Schuster, P. F., Scott, L., Staples, R., Striegl, R. G.,
708 Tretiakov, M., Zhulidov, A. V., Zimov, N., Zimov, S., and Holmes, R. M.: Recent trends in the chemistry of
709 major northern rivers signal widespread Arctic change, *Nat Geosci*, 16, 789–796,
710 <https://doi.org/10.1038/s41561-023-01247-7>, 2023.
- 711 Thomas, R. D. and Rampton, V. N.: Surficial Geology and Geomorphology, Engineer Creek, Yukon
712 Territory, <https://doi.org/10.4095/119068>, 1982a.
- 713 Thomas, R. D. and Rampton, V. N.: Surficial Geology and Geomorphology, North Klondike River, Yukon
714 Territory, <https://doi.org/10.4095/119397>, 1982b.
- 715 Thompson, S. E., Basu, N. B., Lascrain, J., Aubeneau, A., and Rao, P. S. C.: Relative dominance of
716 hydrologic versus biogeochemical factors on solute export across impact gradients, *Water Resour Res*,
717 47, 1–20, <https://doi.org/10.1029/2010WR009605>, 2011.
- 718 Townsend-Small, A., McClelland, J. W., Max Holmes, R., and Peterson, B. J.: Seasonal and hydrologic
719 drivers of dissolved organic matter and nutrients in the upper Kuparuk River, Alaskan Arctic,
720 *Biogeochemistry*, 103, 109–124, <https://doi.org/10.1007/s10533-010-9451-4>, 2011.
- 721 Walvoord, M. A. and Kurylyk, B. L.: Hydrologic Impacts of Thawing Permafrost-A Review, *Vadose Zone*
722 *Journal*, 15, vj2016.01.0010, <https://doi.org/10.2136/vj2016.01.0010>, 2016.
- 723 Webster, A. J., Douglas, T. A., Regier, P., Scheuerell, M. D., and Harms, T. K.: Multi-Scale Temporal Patterns
724 in Stream Biogeochemistry Indicate Linked Permafrost and Ecological Dynamics of Boreal Catchments,
725 *Ecosystems*, 25, 1189–1206, <https://doi.org/10.1007/s10021-021-00709-6>, 2022.
- 726 Woo, M.: Permafrost hydrology in North America, *Atmosphere-Ocean*, 24, 201–234,
727 <https://doi.org/10.1080/07055900.1986.9649248>, 1986.
- 728 Woo, M. and Steer, P.: Slope hydrology as influenced by thawing of the active layer, *Resolute, N.W.T., Can*
729 *J Earth Sci*, 20, 978–986, <https://doi.org/10.1139/e83-087>, 1983.
- 730 Woo, M. K. and Winter, T. C.: The role of permafrost and seasonal frost in the hydrology of northern
731 wetlands in North America, *J Hydrol (Amst)*, 141, 5–31, [https://doi.org/10.1016/0022-1694\(93\)90043-9](https://doi.org/10.1016/0022-1694(93)90043-9),
732 1993.



- 733 Woo, M.-K. and Steer, P.: Runoff Regime of Slopes in Continuous Permafrost Areas, *Canadian Water*
734 *Resources Journal*, 11, 58–68, <https://doi.org/10.4296/cwrj1101058>, 1986.
- 735 Wood, S. N.: Mixed GAM Computation Vehicle with Automatic Smoothness Estimation, 2023.
- 736 Wymore, A. S., Larsen, W., Kincaid, D. W., Underwood, K. L., Fazekas, H. M., McDowell, W. H., Murray, D.
737 S., Shogren, A. J., Speir, S. L., and Webster, A. J.: Revisiting the Origins of the Power-Law Analysis for the
738 Assessment of Concentration-Discharge Relationships, *Water Resour Res*, 59,
739 <https://doi.org/10.1029/2023WR034910>, 2023.
- 740 Surficial Geology dataset: <https://data.geology.gov.yk.ca/Compilation/33>, last access: 5 January 2024.
- 741 Zhi, W. and Li, L.: The Shallow and Deep Hypothesis: Subsurface Vertical Chemical Contrasts Shape
742 Nitrate Export Patterns from Different Land Uses, *Environ Sci Technol*, 54, 11915–11928,
743 <https://doi.org/10.1021/acs.est.0c01340>, 2020.
- 744 Zhi, W., Li, L., Dong, W., Brown, W., Kaye, J., Steefel, C., and Williams, K. H.: Distinct Source Water
745 Chemistry Shapes Contrasting Concentration-Discharge Patterns, *Water Resour Res*, 55, 4233–4251,
746 <https://doi.org/10.1029/2018WR024257>, 2019.
- 747